

# NNP/MM: Fast molecular dynamics simulations with machine learning potentials and molecular mechanics

Raimondas Galvelis,<sup>\*,†</sup> Alejandro Varela-Rial,<sup>†,‡</sup> Stefan Doerr,<sup>†</sup> Roberto Fino,<sup>†</sup> Peter Eastman,<sup>¶</sup> Thomas E. Markland,<sup>¶</sup> John D. Chodera,<sup>§</sup> and Gianni De Fabritiis<sup>\*,†,‡,||</sup>

<sup>†</sup>*Acellera Labs, C/ Doctor Trueta 183, 08005 Barcelona, Spain*

<sup>‡</sup>*Computational Science Laboratory, Universitat Pompeu Fabra, PRBB, C/ Doctor Aiguader 88, 08003 Barcelona, Spain*

<sup>¶</sup>*Department of Chemistry, Stanford University, 327 Campus Drive, Stanford, CA, 94305, USA*

<sup>§</sup>*Computational and Systems Biology Program, Sloan Kettering Institute, Memorial Sloan Kettering Cancer Center, New York, NY 10065, USA*

<sup>||</sup>*Institució Catalana de Recerca i Estudis Avançats (ICREA), Passeig Lluis Companys 23, 08010 Barcelona, Spain*

E-mail: r.galvelis@acellera.com; g.defabritiis@gmail.com

## Abstract

Parametric and non-parametric machine learning potentials have emerged recently as a way to improve the accuracy of bio-molecular simulations. Here, we present NNP/MM, an hybrid method integrating neural network potentials (NNPs) and molecular mechanics (MM). It allows to simulate a part of molecular system with NNP, while

the rest is simulated with MM for efficiency. The method is currently available in ACEMD using OpenMM plugins to optimize the performance of NNPs. The achieved performance is slower but comparable to the state-of-the-art GPU-accelerated MM simulations. We validated NNP/MM by performing MD simulations of four protein-ligand complexes, where NNP is used for the intra-molecular interactions of a ligand and MM for the rest interactions. This shows that NNP can already replace MM for small molecules in protein-ligand simulations. The combined sampling of each complex is 1  $\mu$ s, which are the longest simulations of NNP/MM ever reported. Finally, we have made the setup of the NNP/MM simulations simple and user-friendly.

## 1 Introduction

During the last decade, molecular dynamics (MD) moved from CPU execution to accelerators like graphical processing units (GPUs). Since 2006, CELLMD<sup>1</sup> and later ACEMD started to accelerate biomolecular simulations.<sup>2</sup> Many other MD codes have adapted then to GPUs (e.g. AMBER,<sup>3</sup> GROMACS,<sup>4</sup> NAMD,<sup>5</sup> etc.) or from the beginning have been designed to use GPUs (e.g. OpenMM,<sup>6</sup> HOOMD,<sup>7</sup> TorchMD,<sup>8</sup> etc.). This innovation has increased the speed of MD simulations by two orders of magnitude.<sup>9</sup> During the same period, the accuracy of molecular mechanics (MM) and its force fields (FFs) did not progress at the same speed. For example, the widely used biomolecular FFs (AMBER,<sup>10,11</sup> CHARMM,<sup>12,13</sup> etc.) provide FF parameters for proteins and other common biomolecules, but it is not trivial to obtain accurate parameters for novel drug-like molecules. The recent advance of the neural network potential (NNP) has a potential to change that.<sup>14</sup> NNP is based on an idea that a neural network (NN) is a *universal approximator* (i.e. given a sufficiently large NN and enough training data, any function can be approximated at arbitrary precision), which can be trained to predict the results of quantum mechanics (QM) calculations.<sup>15</sup>

Recently, numerous NNPs have been proposed (SchNet,<sup>16</sup> TensorMol,<sup>17</sup> AIMNet,<sup>18</sup> PhysNet,<sup>19</sup> DimeNet++,<sup>20</sup> OrbNet,<sup>21</sup> PaiNN,<sup>22</sup> SpookyNet,<sup>23</sup> NequIP,<sup>24</sup> OrbNet Denali<sup>25</sup> etc).

One of the most used for organic molecules are ANI<sup>26</sup> and its derivatives<sup>27-30</sup> based on a modified Behler-Parrinello (BP) symmetry function.<sup>31</sup> For example, the benchmarks of ANI-2x on a set of biaryl fragment (typically found in drug molecules) shows a better accuracy than the established general FFs (CGenFF,<sup>32,33</sup> GAFF,<sup>34</sup> OPLS,<sup>35</sup> and OpenFF<sup>36</sup>). The mean absolute error for the entire potential energy profile and rotational barrier heights are 0.5 kcal/mol and 1.0 kcal/mol, respectively,<sup>37</sup> but it is orders of magnitude faster than its reference QM calculations at the DFT level ( $\omega$ B97X/6-31G\*).<sup>30</sup> The calculations take a fraction of a second rather than hours.

However, the BP-type NNPs have several limitations. First, the long-range interactions are not properly accounted for. The NNPs only consider the chemical environment around each atom within a given cut-off distance (5.1 Å for ANI-2x). Second, a limited set of elements is supported (H, C, N, O, F, S, and Cl for ANI-2x). Finally, only neutral molecules can be computed.<sup>30</sup>

Despite the current limitations, NNPs are already improving biomolecular simulations. It has demonstrated that the accuracy of FF for drug-like molecules is improved<sup>38</sup> by reparameterizing dihedral angles with ANI-1x.<sup>27</sup> Alternatively, the hybrid method of NNP and MM (NNP/MM)<sup>39</sup> allows to embed NNP into a simulation. The main idea of NNP/MM is similar to QM/MM:<sup>40,41</sup> an important region of a system is modeled with a more accurate method, while a less accurate and computationally cheaper one is used for the rest of the system. It is important to note that the QM methods explicitly model the electronic structure, while NNP does not. While our approach is similar in a spirit, the main reason to use NNP is to improve the simulation accuracy beyond what is possible with MM.

Recently, Lahey and Rowley<sup>39</sup> have demonstrated the first application of NNP/MM to protein-ligand complexes. NNP/MM is used to refine binding poses and to compute the conformational free energies. Rufa et al.<sup>42</sup> have computed the binding free energies of the Tyk2 congeneric ligand benchmark series<sup>43</sup> using alchemical free energy calculations. Instead of using NNP/MM directly, a non-equilibrium switching scheme has been devised

to correct the standard MM calculations to NNP/MM accuracy. It reduces the errors from 1.0 kcal/mol to 0.5 kcal/mol. Vant et al.<sup>44</sup> have used NNP/MM for the refinement of a protein-ligand complex from cryo-electron microscopy data. The refinement with NNP/MM produces higher-quality models than QM/MM with the semi-empirical PM6 method at lower computational cost. Xu et al.<sup>45</sup> have trained a specialized NNP for zinc and used NNP/MM to simulate zinc-containing proteins. The obtained results are in agreement with QM/MM calculations.

A critical limitation for the wider adoption of NNP/MM is the simulation speed. Despite NNP being much faster than QM, it is still slower than MM. For example, Lahey and Rowley<sup>39</sup> and Vant et al.<sup>44</sup> have reported the simulations speed of 3.4 ns/day and 0.5 ns/day, respectively, on NVIDIA TITAN Xp GPU. Also, the longest reported simulation is just 20 ns.<sup>44</sup>

In this work, we demonstrate the integration of NNP in molecular dynamics simulations by implementing NNP/MM in ACEMD<sup>2</sup> using OpenMM<sup>6</sup> and PyTorch.<sup>46</sup> The implementation is validated by performing MD simulations of four protein-ligand complexes. We have made the set up of NNP/MM as simple as possible to facilitate adaption.

## 2 Methods

In NNP/MM, a system is partitioned into NNP and MM regions similarly to QM/MM.<sup>40,41</sup> The total potential energy ( $V$ ) consists of three terms:

$$V(\vec{r}) = V_{\text{NNP}}(\vec{r}_{\text{NNP}}) + V_{\text{MM}}(\vec{r}_{\text{MM}}) + V_{\text{NNP-MM}}(\vec{r}) \quad (1)$$

where  $V_{\text{NNP}}$  and  $V_{\text{MM}}$  are the potential energies of the NNP and MM regions, respectively.  $V_{\text{NNP-MM}}$  is a coupling term;  $\vec{r}$ ,  $\vec{r}_{\text{NNP}}$ , and  $\vec{r}_{\text{MM}}$  are the atomic position of the entire system, NNP region, and MM region, respectively.

In this work, we adapt the coupling term ( $V_{\text{NNP-MM}}$ ) proposed by Lahey and Rowley:<sup>39</sup>

$$V_{\text{NNP-MM}}(\vec{r}) = \sum_i^{N_{\text{NNP}}} \sum_j^{N_{\text{MM}}} (V_C^{i,j} + V_{LJ}^{i,j}) \quad (2)$$

where  $V_C^{i,j} = \frac{q_i q_j}{4\pi\epsilon_0 r_{ij}}$  is the Coulomb potential,  $V_{LJ}^{i,j} = 4\epsilon_{ij} \left[ \left( \frac{\sigma_{ij}}{r_{ij}} \right)^{12} - \left( \frac{\sigma_{ij}}{r_{ij}} \right)^6 \right]$  is the Lennard-Jones potential and  $N_{\text{NNP}}$  and  $N_{\text{MM}}$  are the number of NNP and MM atoms, respectively;  $q_i$  and  $q_j$  are the atomic charges;  $\epsilon_{ij}$  and  $\sigma_{ij}$  are the Lennard-Jones parameters;  $r_{ij}$  is the distance between the atoms; and  $\epsilon_0$  is the vacuum permittivity (dielectric constant). In the context of QM/MM, this is known as the *mechanical embedding* scheme.<sup>40,41</sup>

NNP/MM is implemented in ACEMD<sup>2</sup> using several software components. OpenMM,<sup>47</sup> a GPU-accelerated MD library, is used to compute MM terms and propagate the MD trajectory. OpenMM-Torch,<sup>48</sup> an OpenMM plugin, is used to compute the NNP term. It uses PyTorch,<sup>46</sup> a ML framework for NN training and inference on GPUs, to load and execute NNP on GPU. TorchANI<sup>49</sup> is used to create the PyTorch model of ANI-2x.<sup>30</sup> TorchMD-NET<sup>50</sup> is used to create the PyTorch models of the the graph network. NNPOps,<sup>51</sup> a library of optimized CUDA kernels for NNP, is used to accelerate critical parts of the computations.

We have optimized the performance of NNP/MM in three ways. First, all the terms of NNP and MM are computed on a GPU. Neither atomic positions nor atomic forces need to be transferred between the CPU and GPU, as it is the case with the original implementation.<sup>39</sup> Second, the featurizer of ANI has been implemented as a custom CUDA kernel and available in the NNPOps library.<sup>51</sup> The original featurizer in TorchANI is implemented using only standard PyTorch operations, which are an inefficient way of performing this calculation. Third, the computation of the atomic networks has been batched to reduce the number of CUDA kernels taking advantage that the same molecule is computed repeatedly. The original TorchANI version is optimized for batch computing (i.e. many molecules are computed simultaneously), while for MD low-latency computing (i.e. one molecule is computed as fast as possible) is necessary. The weights and biases of the atomic NNs are replicated

and batched in the same order as the atoms in a molecule, allowing a GPU to efficiently parallelize the calculation for a single molecule. The implementation of the optimized NNs is available in the NNPOps library <https://github.com/openmm/nnops>).

## 3 Results

### 3.1 Protein-ligand complexes

We have selected four protein-ligand complexes from PDBbind 2019<sup>52,53</sup> following these criteria. First, the ligand contains only elements supported by ANI-2x (H, C, N, O, F, S, and Cl)<sup>30</sup> and no charged functional groups (amonium, carboxylate, etc). Second, the ligand has less than one hundred atoms. Third, the ligand has at least one rotatable bond and the rotamers energies differs by  $>3$  kcal/mol between GAFF2<sup>34</sup> and ANI-2x.<sup>30</sup> We use *Parameterize* tool<sup>38</sup> to detect the rotatable bond, scan the dihedral angles of rotatable bonds and, to compute the relative rotamer energies. The summary of the protein-ligand complexes are given in Table 1 and the ligand structures are shown in Figure 1. Additionally, the energy profiles of the dihedral angle scan of the ligands are available in the supplementary information (Figure S1-S20).

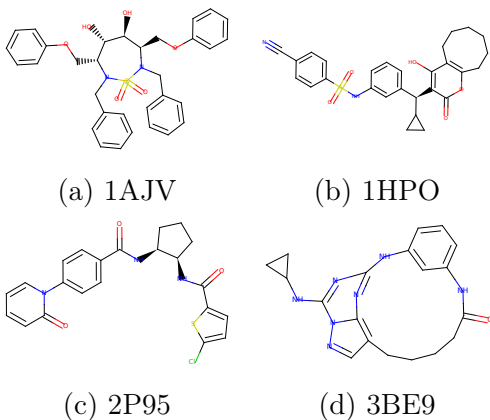


Figure 1: Ligand structures (a-d) of the selected protein-ligand complexes.

The protein-ligand complex preparation and equilibration has been carried out with

Table 1: Summary of protein-ligand complexes.

System	Protein atoms	residues	Ligand atoms	dihedrals	Total atoms
1AJV <sup>54</sup>	3125	198	75	5	38325
1HPO <sup>55</sup>	3133	198	64	6	47712
2P95 <sup>56</sup>	4398	286	50	7	52477
3BE9 <sup>57</sup>	5451	328	48	2	60412

HTMD.<sup>58</sup> Each complex has been simulated with two different methods: MM, where the ligand is parameterized with GAFF2<sup>34</sup> and NNP/MM, where the ligand is modeled with ANI-2x.<sup>30</sup> The protein, in both cases, uses AMBER ff14SB<sup>11</sup> FF. The MD simulations uses the NVT ensemble ( $T = 310\text{ K}$ ), the time step is set to 4.0 fs for the MM simulations, and to 2.0 fs for the NNP/MM simulations. For each combination of a complex and method, 10 independent simulations of 100 ns are performed resulting into the combined sampling of 1  $\mu\text{s}$ . More details are provided in the supplementary information.

### 3.2 Analysis of protein-ligand complexes

All the proteins and ligands maintain their structures in the simulations with both methods (MM and NNP/MM). The protein RMSD fluctuates in the range of 1.8-2.8  $\text{\AA}$  and the residue RMSF have similar magnitudes when comparing the same protein with both methods. The ligand RMSD fluctuates in the range of 0.2-1.7  $\text{\AA}$ . In case of 1AJV and 2P95, there is no significant difference between MM and NNP/MM, but, in case of 1HPO and 3BE9, the fluctuations are larger by  $\sim 0.3\text{ \AA}$  for NNP/MM. The time series pf protein RMSD, residue RMSF, and ligand RMSD are available in the supplementary information (Figure S21-S32). The difference of the ligand RMSD is expect because, as previous works<sup>37,38,42</sup> indicates, ANI-2x models the dihedral angles more accurately than GAFF. Also, it is important to note that our simulations are 50 times longer than previously reported<sup>39</sup> and have not resulted to any non-physical conformation.

The dominant protein-ligand interactions (Figure 2) qualitatively agree between MM and

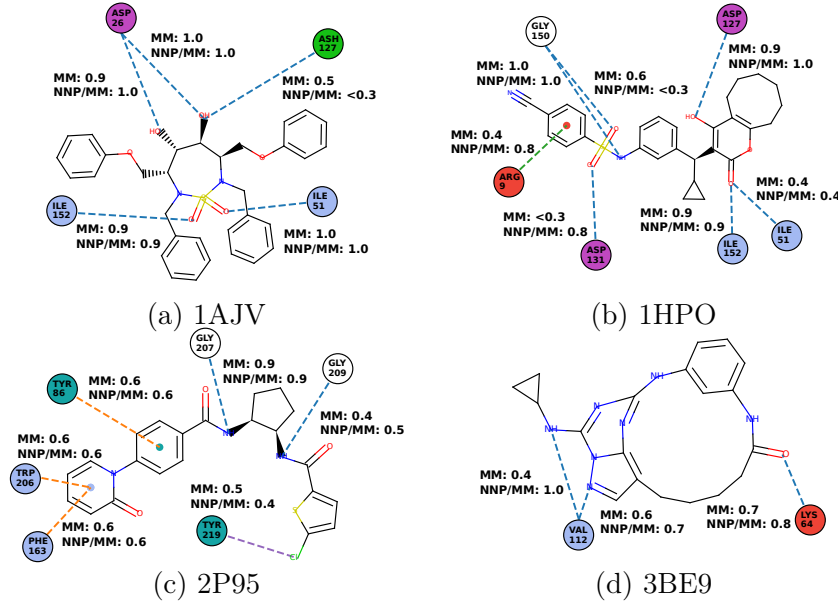


Figure 2: Probabilities of protein-ligand interactions for the different system and methods (a-d). Protein residues are represented as disks (blue: non-polar, green: polar, red: positively charged, magenta: negatively charged, and dark cyan: aromatic). Interactions are depicted as dashed lines (blue: hydrogen bond, green: cation- $\pi$ , orange:  $\pi$ - $\pi$  interaction, and violet:  $\sigma$ -hole). The interactions with probabilities lower than 0.3 are excluded.

NNP/MM for all the complexes. The full list of ligand-protein interactions and technical details are available in the supplementary information (Table S2-S9).

### 3.3 Simulation speed

On average, NNPOps<sup>51</sup> accelerates ANI calculations (energy and forces) 5.9 times (Table 2). There is no strict dependency between the ligand size and the calculation time, which suggests significant overhead is coming from auxiliary operations rather than the computation of NNPs. The overhead mainly comes from PyTorch, which is optimized for batch computing rather low latency.<sup>46</sup>

Overall NNP/MM is sped up 5.1 times (Table 3) on average, when NNPOps<sup>51</sup> is used. Despite of this improvement, NNP/MM is still about an order of magnitude slower than the conventional MM (Table 3), but further optimizations are possible. First, ANI-2x<sup>30</sup> uses an ensemble of 8 NNs. If only one NN could be used, the simulations would be 2.2 times

Table 2: Comparison of ANI-2x inference (energy and forces) time (ms) using the original TorchANI and the TorchANI accelerated with NNPOps (TorchANI/NNPOps). The results obtained with NVIDIA RTX 2080 Ti GPU.

System	TorchANI	TorchANI/NNPOps	Speed-up
1AJV	17.4	3.76	4.6
1HPO	16.5	3.24	5.1
2P95	19.0	2.60	7.3
3BE9	18.1	2.73	6.6
Average			5.9

Table 3: Comparison of MD simulation speed (ns/day) of NNP/MM using the original TorchANI, the TorchANI accelerated with NNPOps (TorchANI/NNPOps), and the TorchANI accelerated with NNPOps and just one model of ANI-2x (1 NN). For reference, MM speed is included. The results obtained with NVIDIA RTX 2080 Ti GPU.

System	NNP/MM (TorchANI)*	NNP/MM (TorchANI/NNPOps)*	NNP/MM (1 NN)*	MM <sup>†</sup>
1AJV	9.19	40.7	101	666
1HPO	9.12	44.6	101	547
2P95	7.93	49.8	96.8	430
3BE9	10.4	50.8	96.5	436

\* 2 fs time step

† 4 fs time step

faster on average (Table 3). Second, the time step for the NNP/MM simulations has to be reduced from 4 fs to 2 fs. If the constraint scheme could be adapted to allow 4 fs timestep, the simulations would be 2 times faster. Finally, not all the software components are already fully optimized. For example, the current implementation of OpenMM-Torch (<https://github.com/openmm/openmm-torch>) performs the NNP and MM calculations on a GPU sequentially, but it would be more efficient to do that concurrently.

We support any NNP model that is based on PyTorch, i.e. we are agnostic with respect the NNP, so when new NNP architectures emerge, it should be trivial to adapt and use them. To demonstrate this, we have performed benchmark simulations with ANI-1x<sup>27</sup> and ANI-1ccx<sup>28</sup> in TorchANI,<sup>49</sup> and TorchMD-NET<sup>50</sup> graph convolution network trained with the ANI-1 data set.<sup>59</sup> The performance benchmarks (Table 4) are available just for 3BE9,

base all the NNPs are limited to 4 elements (H, C, N, and O). TorchMD-NET is slower than ANI however over 5 times more accurate.<sup>50</sup>

Table 4: Comparison of MD simulation speed of ANI-1x and TorchMD-NET and their accuracy in mean absolute error (MAE).<sup>50</sup> The results obtained with NVIDIA RTX 2080 Ti GPU.

System 3BE9	ANI-1x*	TorchMD-NET*
speed (ns/day)	82.7	15.5
accuracy (eV)	0.057	0.010

\* 2 fs time step

### 3.4 Example

ACEMD can be installed with Conda package management system.<sup>60</sup> For dependencies, Conda-forge<sup>61</sup> is used to ensure compatibility with all major Linux distributions (refer to the ACEMD documentation<sup>62</sup> for details at [software.acellera.com](http://software.acellera.com)). For the best performance, it is recommend to have a GPU and its latest drivers installed, but it is possible to run on a CPU only.

A system needs to prepared as for a conventional MM simulation, which includes getting an initial structure, topology, and force field parameters. Note that the NNP atoms needs to be assigned partial charges and Lennard-Jones parameters in order to compute the coupling term correctly. The system preparation can be easily accomplished with HTMD<sup>58</sup> (refer to the HTMD documentation<sup>63</sup> for details). The only additional step is to generate NNP files.

The NNP files can be generated with `prepare-nnp` tool (included with ACEMD). It needs the initial structure file (e.g. `structure.pdb`), a selection of the NNP atoms (e.g. `"resname MOL"`), and a name of NNP

```
prepare-nnp structure.pdb
--selection "resname MOL" --model ANI-2x
```

The tool generates several files including `model.json`. Currently, we plan to support ANI and TorchMD-NET but other models will also be supported in the future. An ACEMD input file needs to be prepared as for a conventional MD simulation (refer to the ACEMD documentation<sup>62</sup> for details). Just one additional line (`nnpfile model.json`) needs to be added to enable NNP/MM and the MD simulation can be performed.

## 4 Conclusion

NNP will play a key role in the near future to improve the accuracy and generality of molecular simulations. Here, we have demonstrated that NNP/MM is a viable method for the simulations of protein-ligand complexes. We expect it to be particularly useful when NNP will be able to handle more atom elements and charges. It can already simulate complex small molecules (like the ligands used in this work) without the need of expensive force field parameterization. NNP/MM is not yet a replacement of QM/MM because of the shortcoming of current NNP compared to DFT, but the performance is many orders of magnitude faster. The simulation speed that we can currently reach is sufficient to start using NNP/MM without being impractical compared to the standard MM. Nevertheless, we expect that it will be improved further by combining state-of-the-art computational libraries (OpenMM,<sup>47</sup> PyTorch,<sup>46</sup> and NNPOps<sup>51</sup>) and specifically optimizing for efficient execution on GPUs.

## Acknowledgement

The authors thank the volunteers of GPUGRID.net for donating computing time. This project has received funding from the Torres-Quevedo Programme from the Spanish National Agency for Research (PTQ-17-09078 / AEI / 10.13039/501100011033) (R.G); the European Union’s Horizon 2020 research and innovation programme under grant agreement No. 823712 (R.G., A.V., R.F.); the Industrial Doctorates Plan of the Secretariat of Universities

and Research of the Department of Economy and Knowledge of the Generalitat of Catalonia (A. V.); the Chan Zuckerberg Initiative DAF (grant number: 2020-219414), an advised fund of Silicon Valley Community Foundation (S.D., P.K.E.) and project PID2020-116564GB-I00 has been funded by MCIN / AEI /10.13039/501100011033. Research reported in this publication was supported by the National Institute of General Medical Sciences (NIGMS) of the National Institutes of Health under award number GM140090 (PKE, TEM, JDC, GDF). The content is solely the responsibility of the authors and does not necessarily represent the official views of the National Institutes of Health. JDC is a current member of the Scientific Advisory Board of OpenEye Scientific Software, Redesign Science, Ventus Therapeutics, and Interline Therapeutics, and has equity interests in Redesign Science and Interline Therapeutics. The Chodera laboratory receives or has received funding from multiple sources, including the National Institutes of Health, the National Science Foundation, the Parker Institute for Cancer Immunotherapy, Relay Therapeutics, Entasis Therapeutics, Silicon Therapeutics, EMD Serono (Merck KGaA), AstraZeneca, Vir Biotechnology, Bayer, XtalPi, Interline Therapeutics, the Molecular Sciences Software Institute, the Starr Cancer Consortium, the Open Force Field Consortium, Cycle for Survival, a Louis V. Gerstner Young Investigator Award, and the Sloan Kettering Institute. A complete funding history for the Chodera lab can be found at <http://choderalab.org/funding>.

## Supporting Information Available

The following files are available free of charge.

- SI.pdf: the energy profiles of the dihedral angle scan of the ligands; detailed performance benchmarks of the simulations; the protein and ligand RMSD and residue RMSF for all the simulations; and the full list of ligand-protein interactions.

## References

- (1) De Fabritiis, G. Performance of the Cell processor for biomolecular simulations. *Computer Physics Communications* **2007**, *176*, 660–664.
- (2) Harvey, M. J.; Giupponi, G.; Fabritiis, G. D. ACEMD: accelerating biomolecular dynamics in the microsecond time scale. *Journal of chemical theory and computation* **2009**, *5*, 1632–1639.
- (3) Salomon-Ferrer, R.; Case, D. A.; Walker, R. C. An overview of the Amber biomolecular simulation package. *Wiley Interdisciplinary Reviews: Computational Molecular Science* **2013**, *3*, 198–210.
- (4) Abraham, M. J.; Murtola, T.; Schulz, R.; Páll, S.; Smith, J. C.; Hess, B.; Lindahl, E. GROMACS: High performance molecular simulations through multi-level parallelism from laptops to supercomputers. *SoftwareX* **2015**, *1*, 19–25.
- (5) Phillips, J. C.; Hardy, D. J.; Maia, J. D.; Stone, J. E.; Ribeiro, J. V.; Bernardi, R. C.; Buch, R.; Fiorin, G.; Hénin, J.; Jiang, W., et al. Scalable molecular dynamics on CPU and GPU architectures with NAMD. *The Journal of chemical physics* **2020**, *153*, 044130.
- (6) Eastman, P.; Pande, V. OpenMM: A hardware-independent framework for molecular simulations. *Computing in science & engineering* **2010**, *12*, 34–39.
- (7) Anderson, J.; Keys, A.; Phillips, C.; Dac Nguyen, T.; Glotzer, S. HOOMD-blue, general-purpose many-body dynamics on the GPU. APS March Meeting Abstracts. 2010; pp Z18–008.
- (8) Doerr, S.; Majewski, M.; Pérez, A.; Krämer, A.; Clementi, C.; Noe, F.; Giorgino, T.; De Fabritiis, G. Torchmd: A deep learning framework for molecular simulations. *Journal of chemical theory and computation* **2021**, *17*, 2355–2363.

(9) Stone, J. E.; Hardy, D. J.; Ufimtsev, I. S.; Schulten, K. GPU-accelerated molecular modeling coming of age. *Journal of Molecular Graphics and Modelling* **2010**, *29*, 116–125.

(10) Cornell, W. D.; Cieplak, P.; Bayly, C. I.; Gould, I. R.; Merz, K. M.; Ferguson, D. M.; Spellmeyer, D. C.; Fox, T.; Caldwell, J. W.; Kollman, P. A. A Second Generation Force Field for the Simulation of Proteins, Nucleic Acids, and Organic Molecules. *J. Am. Chem. Soc.* **1995**, *117*, 5179–5197.

(11) Maier, J. A.; Martinez, C.; Kasavajhala, K.; Wickstrom, L.; Hauser, K. E.; Simmerling, C. ff14SB: improving the accuracy of protein side chain and backbone parameters from ff99SB. *Journal of chemical theory and computation* **2015**, *11*, 3696–3713.

(12) MacKerell, A. D.; Bashford, D.; Bellott, M.; Dunbrack, R. L.; Evanseck, J. D.; Field, M. J.; Fischer, S.; Gao, J.; Guo, H.; Ha, S.; Joseph-McCarthy, D.; Kuchnir, L.; Kuczera, K.; Lau, F. T. K.; Mattos, C.; Michnick, S.; Ngo, T.; Nguyen, D. T.; Prodhom, B.; Reiher, W. E.; Roux, B.; Schlenkrich, M.; Smith, J. C.; Stote, R.; Straub, J.; Watanabe, M.; Wiórkiewicz-Kuczera, J.; Yin, D.; Karplus, M. All-Atom Empirical Potential for Molecular Modeling and Dynamics Studies of Proteins. *J. Phys. Chem. B* **1998**, *102*, 3586–3616.

(13) Huang, J.; MacKerell Jr, A. D. CHARMM36 All-Atom Additive Protein Force Field: Validation Based on Comparison to NMR Data. *J. Comput. Chem.* **2013**, *34*, 2135–2145.

(14) Noé, F.; Tkatchenko, A.; Müller, K.-R.; Clementi, C. Machine learning for molecular simulation. *Annual review of physical chemistry* **2020**, *71*, 361–390.

(15) Behler, J. Constructing high-dimensional neural network potentials: A tutorial review. *International Journal of Quantum Chemistry* **2015**, *115*, 1032–1050.

(16) Schütt, K. T.; Sauceda, H. E.; Kindermans, P.-J.; Tkatchenko, A.; Müller, K.-R. SchNet—A deep learning architecture for molecules and materials. *The Journal of Chemical Physics* **2018**, *148*, 241722.

(17) Yao, K.; Herr, J. E.; Toth, D. W.; Mckintyre, R.; Parkhill, J. The TensorMol-0.1 model chemistry: a neural network augmented with long-range physics. *Chemical science* **2018**, *9*, 2261–2269.

(18) Zubatyuk, R.; Smith, J. S.; Leszczynski, J.; Isayev, O. Accurate and transferable multitask prediction of chemical properties with an atoms-in-molecules neural network. *Science advances* **2019**, *5*, eaav6490.

(19) Unke, O. T.; Meuwly, M. PhysNet: A neural network for predicting energies, forces, dipole moments, and partial charges. *Journal of chemical theory and computation* **2019**, *15*, 3678–3693.

(20) Klicpera, J.; Giri, S.; Margraf, J. T.; Günnemann, S. Fast and Uncertainty-Aware Directional Message Passing for Non-Equilibrium Molecules. *arXiv preprint arXiv:2011.14115* **2020**,

(21) Qiao, Z.; Welborn, M.; Anandkumar, A.; Manby, F. R.; Miller III, T. F. OrbNet: Deep learning for quantum chemistry using symmetry-adapted atomic-orbital features. *The Journal of Chemical Physics* **2020**, *153*, 124111.

(22) Schütt, K. T.; Unke, O. T.; Gastegger, M. Equivariant message passing for the prediction of tensorial properties and molecular spectra. *arXiv preprint arXiv:2102.03150* **2021**,

(23) Unke, O. T.; Chmiela, S.; Gastegger, M.; Schütt, K. T.; Sauceda, H. E.; Müller, K.-R. Spookynet: Learning force fields with electronic degrees of freedom and nonlocal effects. *arXiv preprint arXiv:2105.00304* **2021**,

(24) Batzner, S.; Smidt, T. E.; Sun, L.; Mailoa, J. P.; Kornbluth, M.; Molinari, N.; Kozinsky, B. SE(3)-equivariant graph neural networks for data-efficient and accurate interatomic potentials. *arXiv preprint arXiv:2101.03164* **2021**,

(25) Christensen, A. S.; Sirumalla, S. K.; Qiao, Z.; O'Connor, M. B.; Smith, D. G.; Ding, F.; Bygrave, P. J.; Anandkumar, A.; Welborn, M.; Manby, F. R., et al. OrbNet Denali: A machine learning potential for biological and organic chemistry with semi-empirical cost and DFT accuracy. *arXiv preprint arXiv:2107.00299* **2021**,

(26) Smith, J. S.; Isayev, O.; Roitberg, A. E. ANI-1: an extensible neural network potential with DFT accuracy at force field computational cost. *Chemical science* **2017**, *8*, 3192–3203.

(27) Smith, J. S.; Nebgen, B.; Lubbers, N.; Isayev, O.; Roitberg, A. E. Less is more: Sampling chemical space with active learning. *The Journal of chemical physics* **2018**, *148*, 241733.

(28) Smith, J. S.; Nebgen, B. T.; Zubatyuk, R.; Lubbers, N.; Devereux, C.; Barros, K.; Tretiak, S.; Isayev, O.; Roitberg, A. E. Approaching coupled cluster accuracy with a general-purpose neural network potential through transfer learning. *Nature communications* **2019**, *10*, 1–8.

(29) Stevenson, J. M.; Jacobson, L. D.; Zhao, Y.; Wu, C.; Maple, J.; Leswing, K.; Harder, E.; Abel, R. Schrödinger-ANI: An Eight-Element Neural Network Interaction Potential with Greatly Expanded Coverage of Druglike Chemical Space. *arXiv preprint arXiv:1912.05079* **2019**,

(30) Devereux, C.; Smith, J. S.; Davis, K. K.; Barros, K.; Zubatyuk, R.; Isayev, O.; Roitberg, A. E. Extending the Applicability of the ANI Deep Learning Molecular Potential to Sulfur and Halogens. *Journal of Chemical Theory and Computation* **2020**, *16*, 4192–4202.

(31) Behler, J.; Parrinello, M. Generalized neural-network representation of high-dimensional potential-energy surfaces. *Physical review letters* **2007**, *98*, 146401.

(32) Vanommeslaeghe, K.; Hatcher, E.; Acharya, C.; Kundu, S.; Zhong, S.; Shim, J.; Darrian, E.; Guvench, O.; Lopes, P.; Vorobyov, I., et al. CHARMM general force field: A force field for drug-like molecules compatible with the CHARMM all-atom additive biological force fields. *Journal of computational chemistry* **2010**, *31*, 671–690.

(33) Vanommeslaeghe, K.; Raman, E. P.; MacKerell Jr, A. D. Automation of the CHARMM General Force Field (CGenFF) II: assignment of bonded parameters and partial atomic charges. *Journal of chemical information and modeling* **2012**, *52*, 3155–3168.

(34) Wang, J.; Wolf, R. M.; Caldwell, J. W.; Kollman, P. A.; Case, D. A. Development and testing of a general amber force field. *Journal of computational chemistry* **2004**, *25*, 1157–1174.

(35) Jorgensen, W. L.; Tirado-Rives, J. Potential energy functions for atomic-level simulations of water and organic and biomolecular systems. *Proceedings of the National Academy of Sciences* **2005**, *102*, 6665–6670.

(36) Mobley, D. L.; Bannan, C. C.; Rizzi, A.; Bayly, C. I.; Chodera, J. D.; Lim, V. T.; Lim, N. M.; Beauchamp, K. A.; Slochower, D. R.; Shirts, M. R., et al. Escaping atom types in force fields using direct chemical perception. *Journal of chemical theory and computation* **2018**, *14*, 6076–6092.

(37) Lahey, S.-L. J.; Thien Phuc, T. N.; Rowley, C. N. Benchmarking Force Field and the ANI Neural Network Potentials for the Torsional Potential Energy Surface of Biaryl Drug Fragments. *Journal of Chemical Information and Modeling* **2020**,

(38) Galvelis, R.; Doerr, S.; Damas, J. M.; Harvey, M. J.; De Fabritiis, G. A Scalable Molecular Force Field Parameterization Method Based on Density Functional Theory

and Quantum-Level Machine Learning. *Journal of chemical information and modeling* **2019**, *59*, 3485–3493.

(39) Lahey, S.-L. J.; Rowley, C. N. Simulating protein–ligand binding with neural network potentials. *Chemical Science* **2020**, *11*, 2362–2368.

(40) Lin, H.; Truhlar, D. G. QM/MM: what have we learned, where are we, and where do we go from here? *Theoretical Chemistry Accounts* **2007**, *117*, 185–199.

(41) Senn, H. M.; Thiel, W. QM/MM methods for biomolecular systems. *Angewandte Chemie International Edition* **2009**, *48*, 1198–1229.

(42) Rufa, D. A.; Macdonald, H. E. B.; Fass, J.; Wieder, M.; Grinaway, P. B.; Roitberg, A. E.; Isayev, O.; Chodera, J. D. Towards chemical accuracy for alchemical free energy calculations with hybrid physics-based machine learning/molecular mechanics potentials. *BioRxiv* **2020**,

(43) Wang, L.; Wu, Y.; Deng, Y.; Kim, B.; Pierce, L.; Krilov, G.; Lupyan, D.; Robinson, S.; Dahlgren, M. K.; Greenwood, J., et al. Accurate and reliable prediction of relative ligand binding potency in prospective drug discovery by way of a modern free-energy calculation protocol and force field. *Journal of the American Chemical Society* **2015**, *137*, 2695–2703.

(44) Vant, J. W.; Lahey, S.-L. J.; Jana, K.; Shekhar, M.; Sarkar, D.; Munk, B. H.; Kleinekathöfer, U.; Mittal, S.; Rowley, C.; Singharoy, A. Flexible Fitting of Small Molecules into Electron Microscopy Maps Using Molecular Dynamics Simulations with Neural Network Potentials. *Journal of Chemical Information and Modeling* **2020**,

(45) Xu, M.; Zhu, T.; Zhang, J. Z. Automatically Constructed Neural Network Potentials for Molecular Dynamics Simulation of Zinc Proteins. *Frontiers in Chemistry* **2021**, *9*.

(46) Paszke, A.; Gross, S.; Massa, F.; Lerer, A.; Bradbury, J.; Chanan, G.; Killeen, T.; Lin, Z.; Gimelshein, N.; Antiga, L., et al. Pytorch: An imperative style, high-performance deep learning library. *arXiv preprint arXiv:1912.01703* **2019**,

(47) Eastman, P.; Swails, J.; Chodera, J. D.; McGibbon, R. T.; Zhao, Y.; Beauchamp, K. A.; Wang, L.-P.; Simmonett, A. C.; Harrigan, M. P.; Stern, C. D., et al. OpenMM 7: Rapid development of high performance algorithms for molecular dynamics. *PLoS computational biology* **2017**, *13*, e1005659.

(48) Eastman, P. OpenMM-Torch. <https://github.com/openmm/openmm-torch>, 2021.

(49) Gao, X.; Ramezanghorbani, F.; Isayev, O.; Smith, J.; Roitberg, A. TorchANI: A Free and Open Source PyTorch Based Deep Learning Implementation of the ANI Neural Network Potentials. **2020**,

(50) EQUIVARIANT TRANSFORMERS FOR NEURAL NETWORK BASED MOLECULAR POTENTIALS. <https://openreview.net/pdf?id=zNHzqZ9wrRB> **2021**,

(51) Eastman, P.; Galvelis, R. NNPOps. <https://github.com/openmm/nnpoops>, 2021.

(52) Wang, R.; Fang, X.; Lu, Y.; Wang, S. The PDBbind database: Collection of binding affinities for protein- ligand complexes with known three-dimensional structures. *Journal of medicinal chemistry* **2004**, *47*, 2977–2980.

(53) Liu, Z.; Su, M.; Han, L.; Liu, J.; Yang, Q.; Li, Y.; Wang, R. Forging the basis for developing protein–ligand interaction scoring functions. *Accounts of chemical research* **2017**, *50*, 302–309.

(54) Bäckbro, K.; Löwgren, S.; Österlund, K.; Atepo, J.; Unge, T.; Hultén, J.; Bonham, N. M.; Schaal, W.; Karlén, A.; Hallberg, A. Unexpected binding mode of a cyclic sulfamide HIV-1 protease inhibitor. *Journal of medicinal chemistry* **1997**, *40*, 898–902.

(55) Skulnick, H. I.; Johnson, P. D.; Aristoff, P. A.; Morris, J. K.; Lovasz, K. D.; Howe, W. J.; Watenpaugh, K. D.; Janakiraman, M. N.; Anderson, D. J.; Reischer, R. J., et al. Structure-based design of nonpeptidic HIV protease inhibitors: the sulfonamide-substituted cyclooctylpyranones. *Journal of medicinal chemistry* **1997**, *40*, 1149–1164.

(56) Qiao, J. X.; Chang, C.-H.; Cheney, D. L.; Morin, P. E.; Wang, G. Z.; King, S. R.; Wang, T. C.; Rendina, A. R.; Luettgen, J. M.; Knabb, R. M., et al. SAR and X-ray structures of enantiopure 1, 2-cis-(1R, 2S)-cyclopentyldiamine and cyclohexyldiamine derivatives as inhibitors of coagulation Factor Xa. *Bioorganic & medicinal chemistry letters* **2007**, *17*, 4419–4427.

(57) Nie, Z.; Perretta, C.; Erickson, P.; Margosiak, S.; Lu, J.; Averill, A.; Almassy, R.; Chu, S. Structure-based design and synthesis of novel macrocyclic pyrazolo [1, 5-a][1, 3, 5] triazine compounds as potent inhibitors of protein kinase CK2 and their anticancer activities. *Bioorganic & medicinal chemistry letters* **2008**, *18*, 619–623.

(58) Doerr, S.; Harvey, M.; Noé, F.; De Fabritiis, G. HTMD: high-throughput molecular dynamics for molecular discovery. *Journal of chemical theory and computation* **2016**, *12*, 1845–1852.

(59) Smith, J. S.; Isayev, O.; Roitberg, A. E. ANI-1, A data set of 20 million calculated off-equilibrium conformations for organic molecules. *Scientific data* **2017**, *4*, 1–8.

(60) Conda. <https://docs.conda.io/>.

(61) conda-forge. <https://conda-forge.org/>.

(62) ACEMD documentation. <https://software.acellera.com/docs/latest/acemd3>.

(63) HTMD documentation. <https://software.acellera.com/docs/latest/htmd>.

# Graphical TOC Entry

